

Structure of the solvated yttrium(III) ion in the oxygen donor solvents dimethyl sulfoxide, *N,N*-dimethylformamide and *N,N'*-dimethylpropyleneurea and crystal structures of $[Y(OSMe_2)_8]I_3$ and $[Y(OCN_2Me_2(CH_2)_3)_6]I_3$

Patric Lindqvist-Reis,^a Jan Näslund,^b Ingmar Persson^b and Magnus Sandström^{ac*}

^a Department of Chemistry, Royal Institute of Technology, S-100 44 Stockholm, Sweden

^b Department of Chemistry, Swedish University of Agricultural Sciences, P.O. Box 7015, S-750 07 Uppsala, Sweden

^c Department of Structural Chemistry, Arrhenius Laboratory, Stockholm University, 106 91 Stockholm, Sweden

Received 6th January 2000, Accepted 26th June 2000

Published on the Web 26th July 2000

The structure of the solvated yttrium(III) ion in the oxygen donor solvents dimethyl sulfoxide, *N,N*-dimethylformamide and *N,N'*-dimethylpropyleneurea, $OCN_2Me_2(CH_2)_3$, has been studied by means of XAFS and large angle X-ray scattering. The yttrium(III) ion co-ordinates eight solvent molecules in dimethyl sulfoxide and *N,N*-dimethylformamide solution with the mean Y–O bond distance 2.36(1) Å. The slightly asymmetric distribution was modelled by the cumulant expansion method for the XAFS data. The Y...S distance of the $[Y(OSMe_2)_8]^{3+}$ ion in dimethyl sulfoxide solution was found to be 3.54(1) Å, corresponding to a mean Y–O–S angle of 132°. For the $[Y(OCHNMe_2)_8]^{3+}$ ion in *N,N*-dimethylformamide the Y...C distance is 3.34(1) Å, giving a Y–O–C angle of 133°. In *N,N'*-dimethylpropyleneurea solution the steric effect of the bulky solvent molecules reduces the co-ordination number to six and the mean Y–O bond distance to 2.24(1) Å. The mean Y...C distance at 3.48(2) Å agrees with an analysis of the angular-sensitive multiple scattering contributions, which gave a Y–O–C angle of about 165°. The crystal structures of $[Y(OCN_2Me_2(CH_2)_3)_6]I_3$ and $[Y(OSMe_2)_8]I_3$, determined by X-ray diffraction at room temperature, show the ionic radii of yttrium(III) to increase about 0.12 Å from six to eight co-ordination.

Introduction

Few structural investigations have been made of the solvated yttrium(III) ion in non-aqueous solution.¹ Previous large angle X-ray scattering (LAXS) studies of yttrium(III) nitrate and chloride in dimethyl sulfoxide solutions indicated a co-ordination number of eight, but with inner-sphere complex formation of the anions.² Owing to the similarity in size and chemical behaviour, the structural chemistry of yttrium(III) is often compared with that of the heavy lanthanide(III) ions. In particular the erbium(III) ion has been used for isostructural comparisons with yttrium(III) in aqueous solution,^{2,3} although the isostructural crystalline hydrates of holmium(III) show even closer similarities in bond distances.⁴

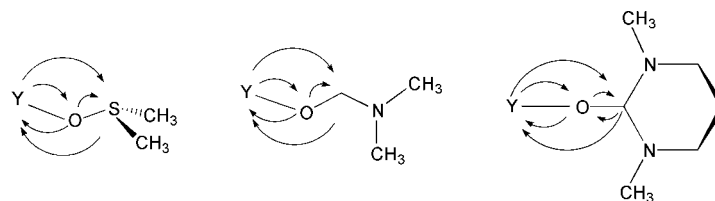
Crystal structure studies of yttrium(III) hydrates are numerous and show a variety of co-ordination numbers. The characteristic mean Y–O bond distance is typically 2.35–2.38 Å for co-ordination of eight oxygen atoms, although no structure with a regular co-ordination figure (square antiprism or dodecahedron) has been found.⁵ Nine-co-ordination gives a slightly longer average Y–O bond distance, with an increase of about 0.06 Å as estimated from Shannon's effective ionic radii,⁶ as in the tricapped trigonal prism in the $[Y(H_2O)_9][CF_3SO_3]_3$ structure with two groups of bond distances, 6×2.344 and 3×2.525 Å.⁷ For six-co-ordination, which probably occurs in the $[Y(H_2O)_6][ClO_4]_3$ compound,⁸ the Y–O bond distance should be about 0.12 Å shorter than for eight-co-ordination, according to the difference in Shannon's ionic radii.⁶ For non-aqueous solvents only a few crystal structures are known with fully solvated lanthanide(III) ions, e.g. the dimethyl sulfoxide solvates $[La(Me_2SO)_8][Cr(NCS)_6]$, $[Gd(Me_2SO)_8][Fe(CN)_6]$, and the *N,N*-dimethylformamide solvate $[Nd(OCHNMe_2)_8][W_4Ag_5S_{16}]$, all with eight oxygen atoms co-ordinated in distorted square antiprisms.^{9–11}

In solution, the balance between the electrostatic bonding and steric ligand–ligand repulsion effects seems to control the co-ordination number of monodentate oxygen donor ligands for these large ions. For the lanthanide(III) ions in aqueous solution there is considerable evidence showing a change in the hydration number from nine to eight with decreasing size in the middle of the series.¹² The energy difference between the different conformations is small, allowing rapid interconversions.¹³ In aqueous solution, yttrium(III) is hydrated by eight water molecules with a slightly asymmetric distribution of the Y–O bond distances around 2.368(5) Å.⁵ The width of the distribution implied a configurational disorder of about 0.1 Å in addition to the thermal disorder.⁵

In this work the structure of the solvated yttrium(III) ion is studied in the oxygen donor solvents dimethyl sulfoxide, *N,N*-dimethylformamide and *N,N'*-dimethylpropyleneurea. The latter is an aprotic solvent with high relative permittivity 4.23 D, high permittivity, $\epsilon = 36.1$,¹⁴ and the D_s value of 34 is high for an oxygen donor,¹⁵ compared with 27.5 for dimethyl sulfoxide and 24 for *N,N*-dimethylformamide.¹⁶ This shows that *N,N'*-dimethylpropyleneurea co-ordinates strongly to both hard and soft metal ions. Both *N,N'*-dimethylpropyleneurea and *N,N*-dimethylformamide co-ordinate *via* the carbonyl oxygen atom. However, due to the bulkiness of the *N,N'*-dimethylpropyleneurea molecule (*cf.* Scheme 1) a low co-ordination number is expected, as already found for the lanthanum(III) and bismuth(III) ions.¹⁷ One aim of the present work is to compare the co-ordination mode and geometry of the little investigated solvent *N,N'*-dimethylpropyleneurea with that of the two well known aprotic oxygen donor solvents dimethyl sulfoxide and *N,N*-dimethylformamide. Another is to establish the variation in the Y–O distance with the co-ordination number, in particular for six-co-ordination. For this purpose, structure studies in solution are desirable in order to avoid possible effects on the

Table 1 Concentration (mol dm⁻³), density and linear adsorption coefficient of the solutions used for in the XAFS and LAXS experiments

Sample	[Y ³⁺]	[CF ₃ SO ₃ ⁻]	[Solvent]	D/g cm ⁻³
^a Y(CF ₃ SO ₃) ₃ in Me ₂ SO L1	0.98	2.94	11.2	1.40
^a (CF ₃ SO ₃) ₃ in Me ₂ NCHO L2	0.96	2.88	9.8	1.23
^a Y(CF ₃ SO ₃) ₃ in <i>N,N'</i> -dimethylpropyleneurea L3	0.25	0.75	7.8	1.15
^b Y(CF ₃ SO ₃) ₃ in Me ₂ SO L4	0.71	2.13	12.0	1.31

^a XAFS, ^b LAXS, $\mu = 111 \text{ mm}^{-1}$.**Scheme 1** The co-ordination modes of dimethyl sulfoxide (left), *N,N*-dimethylformamide (centre) and *N,N'*-dimethylpropyleneurea (right) to yttrium(III). The most important pathways in the corresponding XAFS spectra are found to be the single backscattering (Y–O, Y···S/C) and the 3-leg multiple scattering (Y–O–S/Y–O–C) paths. For the close to linear (≈ 165 – 170°) Y–O–C co-ordination of *N,N'*-dimethylpropyleneurea the 4-leg Y–O–C–O scattering path is also important.

co-ordination by the packing of ions in a solid. On the other hand, crystal structures of solvates are useful for the construction of models for the solvated ions in solution, and are especially valuable for the interpretation of XAFS data. Two crystalline solvates, $[\text{Y}(\text{Me}_2\text{SO})_8]\text{I}_3$ and $[\text{Y}(\text{OCN}_2\text{Me}_2(\text{CH}_2)_3)_6]\text{I}_3$, have been structurally characterised by X-ray diffraction in the present work. Both the XAFS and LAXS techniques were used for the structure studies of yttrium solvates in solution.

The low-energy part of the XAFS spectrum (XANES), which has a considerable contribution from multiple scattering (MS) and therefore contains information about the co-ordination number around the absorbing yttrium atom, is often useful for qualitative comparisons. In the high-energy region (EXAFS) the single back scattering (SS) from the first and second co-ordination shells is dominant and can be analysed quantitatively, but also the three-leg M–O–S or M–O–C scattering paths were found to give significant contributions and used to extract information about the configuration of the ligands. The basis for the comparisons between XAFS spectra of molecular species in solution and in the solid state is generally that contributions from long-range non-bonded interactions are rapidly damped in the EXAFS region because of the large variations in their distances (high Debye–Waller factors). Such interactions are often better represented in LAXS studies for which overlap with contributions from multiple scattering is not a problem. However, concentrated solutions are required since all interatomic distances contribute to the scattering.¹⁸ In the present work a LAXS study was made of the solvated yttrium(III) ion in dimethyl sulfoxide solution which allows the Y···S distance and thus the mean Y–O–S angle accurately to be determined.

Careful evaluation of both XAFS and LAXS data can give the interatomic distances of the dominating interactions with high accuracy, in particular the first-shell metal–oxygen bond distances. In this work we extend the model function for the XAFS data to include all the important scattering paths within the first and second co-ordination shells. As discussed elsewhere,⁵ comparing XAFS spectra for solid solvates and solutions allows higher accuracy in the determination of co-ordination numbers and geometries.

Experimental

Sample preparation

Solutions of Y(CF₃SO₃)₃ in dimethyl sulfoxide, *N,N*-dimethylformamide and *N,N'*-dimethylpropyleneurea. Anhydrous Y(CF₃SO₃)₃ was obtained after dissolving yttrium(III) oxide in

trifluoromethanesulfonic acid with some water added, followed by evaporation and drying at 200 °C. A TGA analysis confirmed complete dryness after this procedure.¹⁹ Solutions were prepared by dissolving the anhydrous salt in dimethyl sulfoxide (Merck), *N,N*-dimethylformamide (Fluka, analytical grade) and *N,N'*-dimethylpropyleneurea (BASF) under a nitrogen atmosphere. The solvents were freshly distilled over calcium hydride (Fluka) before use. Conductometric measurements (Methrom 644) of Y(CF₃SO₃)₃ in the three solvents showed complete dissociation for concentrations up to 0.1 mol dm⁻³. Only for the saturated 0.3 mol dm⁻³ *N,N'*-dimethylpropyleneurea solution **L3** (Table 1) was some ion pair association indicated. EDTA titration with xylenol orange as indicator was used to determine the yttrium concentration,²⁰ and cation exchange (Dowex 50W-X8, H⁺ form), followed by standard acid–base titration, for determining the anion concentration. The solution densities were measured with an Anton Paar DMA 35 densitometer. Concentrations and densities for the solutions used in the XAFS and LAXS studies are given in Table 1.

Crystalline compounds. Evaporation of the yttrium trifluoromethanesulfonate solutions in a desiccator under vacuum only yielded crystals for the dimethyl sulfoxide solution. These crystals could not, however, be used for structure determination as they gave only a few strong reflections. The reason is probably extensive disorder of the triflate ions and the co-ordinated dimethyl sulfoxide molecules. However, with iodide, which does not co-ordinate to the hard yttrium(III) ion, single crystals of X-ray quality could be obtained by slowly cooling saturated solutions of anhydrous YI₃ (Aldrich) in dimethyl sulfoxide and *N,N'*-dimethylpropyleneurea. The yttrium and iodide contents of these crystalline compounds, $[\text{Y}(\text{OSMe}_2)_8]\text{I}_3$ **1** and $[\text{Y}(\text{OCN}_2\text{Me}_2(\text{CH}_2)_3)_6]\text{I}_3$ **2**, were determined by EDTA and cation exchange, respectively (as above). IR spectra of **1** (diluted in polyethylene for far-IR and KBr for mid-IR) were recorded on a Bio-Rad FTS 6000 spectrometer, and Raman spectra of **1** and **2** with a Renishaw System 1000 spectrometer equipped with a microscope (Leica DMLM), a diode laser (782 nm) and a Peltier-cooled CCD detector. The band positions and assignments are as follows: Compound **1**: IR 3009 (sh), 2980s, 2900s, 2811m (CH₃ stretching); 1436 (sh), 1408s, 1352 (sh), 1316s, 1295 (sh), 1026vs (CH₃ bend); 963s (SO str); 916w (CH₃ bend); 712s, 678w (CS str); 438 (sh), 428 (sh), 417m, 397 (sh) (YO str); 349m (CSC bend); 318m, 219m, 196 (sh) (CSO bend) and 117w (YOS bend); Raman: 3007 (sh), 2980w, 2902m (CH₃ str); 1416m, 1316w, 1295w, 1059m, 1025 (sh), 1004m

(CH₃ bend); 964m (SO str); 916w (CH₃ bend); 712s, 678vs (CS str); 427 (sh), 414w, 402 (sh) (YO str); 349s (CSC bend); 314s, 198m (CSO bend) and 118w (YOS bend). Compound **2**: Raman: 2961w, 2941w, 2918w, 2867m, 2794w (CH₃ str); 1490 (sh), 1484w, 1474m, 1458m, 1410w, 1398m, 1325 (sh), 1318m, 1293m, 1287 (sh), 1233m, 1200w, 1138w, 1103w, 1063m, 1043m, 948s, 919m, 888w, 736vs, 728s, 710w, 599vs, 493s, 439s, 361w, 344w, 314w, 220 (sh), 201w and 149w. The abbreviations are sh shoulder, v very, s strong, m medium and w weak.

X-Ray crystallography

Selected crystallographic data and details of structure refinement for compounds **1** and **2** are given in Table 2. A Bruker SMART diffractometer, with a CCD area detector (crystal to detector distance 5.00 cm) and Mo-K α radiation ($\lambda = 0.7107$ Å), was used. For both compounds a full sphere of data consisting of 1375 frames was collected, and the first 50 frames were remeasured at the end of the data collection to monitor instrument and crystal stability. Intensity decay was negligible. The cell parameters were refined using 6198 and 5989 reflections ($I > 2\sigma$) for **1** and **2**, respectively. Data reduction, empirical absorption correction and structure determination (by direct methods) were performed using the Bruker standard software.²¹ All hydrogen atoms could be located in the Fourier difference map for **2**, but not for **1**, before using constraint parameters (HFIX). Three of the dimethyl sulfoxide ligands in **1** are disordered with an inverted orientation of the sulfur atom.

CCDC reference number 186/2059.

See <http://www.rsc.org/suppdata/dt/b0/b005119p/> for crystallographic files in .cif format.

X-Ray absorption fine structure

Measurements. Yttrium K-edge X-ray absorption spectra were recorded at the Stanford Synchrotron Radiation Laboratory (SSRL) using the wiggler beam line 4-1, which was equipped with a Si[220] double crystal monochromator. The SSRL operates at 3.0 GeV and a maximum current of 100 mA. The data collection was performed in transmission mode at ambient temperature, and higher order harmonics were reduced by detuning the second monochromator crystal to reflect 50% of maximum intensity at the end of the scans. The solids were diluted with boron nitride to give an edge step of about one unit in the logarithmic intensity ratio. The solutions were kept in cells with thin glass windows (≈ 35 μ m) and Teflon or Viton spacers (1–5 mm). The energy scale of the X-ray absorption spectra was calibrated by assigning the first inflection point of the metal K-edge of a simultaneously measured yttrium foil to 17038 eV. For each sample 3 or 4 scans were averaged, giving satisfactory data (k^3 -weighted) up to $k = 15.5$ Å⁻¹. The EXAFSPAK program package was used for these preliminary steps of the data treatment.²²

Data analysis. The XAFS oscillations were obtained after performing standard procedures for pre-edge subtraction, normalisation and spline removal by means of the WinXAS software.²³ Model functions were calculated using *ab initio* calculated phase and amplitude parameters obtained by the FEFF 8 program.^{24,25} The input to the FEFF 8 program was prepared from an appropriate crystal structure with a solvated metal ion, to contain all ligand atoms within a radius up to 5 Å from the metal centre. For the dimethyl sulfoxide and *N,N'*-dimethylpropyleneurea solutions the crystal structures of **1** and **2** were used, respectively, and for the *N,N*-dimethylformamide (dmf) solution the crystal structure of [Nd(dmf)₈]_n·[W₄Ag₅S₁₆]_n with yttrium replacing neodymium in the metal atom position.¹¹ In the output, close distances from the same kind of back-scattering atoms were described as a co-ordination shell with a single distance parameter. With this assumption model functions for the single back scattering (SS)

from the first and second co-ordination shells and for the most important multiple scattering (MS) paths (Scheme 1) were curve-fitted in k space (2.0–15.5 Å⁻¹) to the k^3 -weighted data. The models used described the main peaks in the Fourier transforms and Fourier filtering (0.7–4.2 Å) was only necessary for the *N,N'*-dimethylpropyleneurea solution in order to eliminate back-scattering contributions from longer pathways.

For a solvated complex in solution, normally only pathways with rather limited lengths need to be considered, in particular for high co-ordination numbers and flexible ligand conformations. Within the co-ordinated solvent molecules well defined back-scattering pathways can occur, and for the *N,N'*-dimethylpropyleneurea ligands the Y...C, Y–O–C and Y–O–C–O scattering path lengths are similar and were correlated by keeping a fixed difference (in the final model corresponding to Y–O–C 167°) between their distances, and by using the same Debye–Waller factor for all three pathways.

The angle dependence of the MS focusing effect was investigated by generating theoretical XAFS spectra varying the Y–O–C angle from 180 to 150° for an octahedral Y(O–C)₆ complex with Y–O and O–C distances of 2.24 and 1.27 Å, respectively, including all SS and MS paths of importance (amplitude > 2.5%) for $r < 5.0$ Å and using an overall Debye–Waller factor of 0.0065 Å².

The strategy for obtaining the structure and co-ordination of the solvated ions in solution is: (1) determine the Y–O bond distance and use the strong correlation between ionic radii and co-ordination number⁶ to obtain the solvation number (as discussed in the Introduction), and (2) compare XAFS spectra of solvates in crystal structures to identify similarities in the edge structure and the multiple scattering within the first co-ordination sphere, which can be characteristic for a certain co-ordination figure. Moreover, a closely related crystalline solvate can make it possible to obtain a reliable and transferable value for the amplitude reduction factor, S_0^2 , under the experimental condition used. In favourable cases, this may allow the accuracy in the determination of the co-ordination number to be better than ± 0.5 units. Attempts to determine co-ordination numbers without using well defined calibration compounds generally give very large errors, up to the order of $\pm 25\%$,²⁶ since the co-ordination number is directly proportional to the amplitude reduction factor, and also strongly correlated to the Debye–Waller factor.

Co-ordination shell asymmetry was considered by r -space fitting of the Y–O shell in the range up to 3 Å of the Fourier transformed XAFS data (k range 2.0–15.5 Å⁻¹, no window function) by means of the cumulant expansion method, including the third cumulant, C_3 , which compensates for phase shifts in the XAFS function.^{27,28} The ΔE_0 values obtained from the model with symmetric distribution were kept fixed (because of the strong correlation between the bond lengths and ΔE_0) during the refinements using the cumulant expansion. The shift of the threshold energy, ΔE_0 , was close to zero for all samples, and the amplitude reduction factor, S_0^2 , was found to be in the range 0.88–0.94.

Large angle X-ray scattering

Mo-K α ($\lambda = 0.7107$ Å) radiation was used in a θ – θ diffractometer of Bragg–Brentano type for the LAXS measurements on the Y(CF₃SO₃)₃ dimethyl sulfoxide solution. Intensity data were collected at 450 discrete θ values for scattering angles $1 < \theta < 65^\circ$, corresponding to 0.3–16 Å⁻¹ for the scattering variable $s = (4\pi \sin \theta)/\lambda$. Two scans, each accumulating 100,000 counts at every preset angle, were averaged giving a statistical error of about 0.3% in the measured intensities. Details of the data collection and the analysis procedure, and the most important expressions used in the treatment of LAXS data, are given elsewhere.²⁹

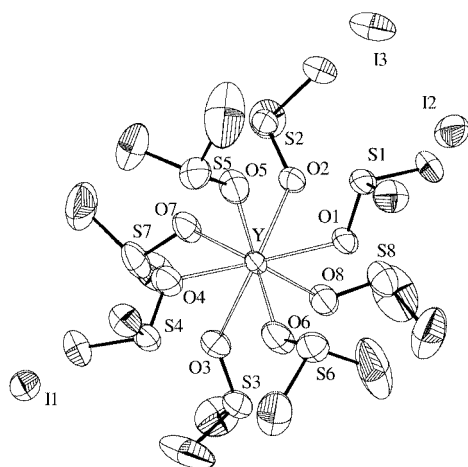


Fig. 1 Molecular structure of $[Y(OSMe_2)_8]I_3$ **1**. Thermal ellipsoids are at 40% probability. Distances (Å) are: Y–O(1) 2.368(3), Y–O(2) 2.363(3), Y–O(3) 2.367(4), Y–O(4) 2.367(4), Y–O(5) 2.320(4)*, Y–O(6) 2.311(4)*, Y–O(7) 2.352(4), Y–O(8) 2.314(4)* (* apparent shortening due to disorder). The mean Y...S distance is 3.53 Å.

The model function was obtained by introducing bond distances and thermal parameters for the trifluoromethanesulfonate anion (staggered conformation),³⁰ and the dimethyl sulfoxide molecule at values previously obtained in similar experiments.³¹ The structure of the solvated ion was modelled as a square antiprism of oxygen atoms around yttrium and an independent mean Y...S distance to a second shell. Optimisation of the model function was made by least-squares refinement of the Y–O and Y...S distances and corresponding thermal parameters for fixed co-ordination numbers. A model with nine oxygen atoms in a tricapped trigonal prism was also tested. The KURVLR program was used for treatment of the LAXS data and the STEPLR program for least-squares refinements of the structure parameters.^{32,33}

Results and discussion

Crystal structures of $[Y(OSMe_2)_8]I_3$ **1** and $[Y(OCN_2Me_2(CH_2)_3)_6]I_3$ **2**

In the dimethyl sulfoxide solvate **1** the eight co-ordinated oxygen atoms form a distorted square antiprism (Fig. 1). Three of the dimethyl sulfoxide molecules are disordered with inverted conformations giving two alternative positions for the sulfur atoms S5, S6 and S8, which are located about 0.6 Å above and below a plane through the oxygen and the methyl carbon atoms. The occupancy factors were refined to 0.760(6), 0.538(7) and 0.886(5) for the main positions of the three sulfur atoms, respectively. The inversion of a dimethyl sulfoxide molecule also leads to two unresolved oxygen positions, which make the apparent Y–O bond distance too short, as also was found for the two dimethyl sulfoxide ligands in $[Y(H_2O)_6(OSMe_2)_2]Cl_3$.³⁴ The effect of disorder is also seen in the S–O bond distance within the dimethyl sulfoxide ligands. For the five non-disordered ligands the mean value is 1.52 Å, as expected for O-co-ordination,³⁵ but smaller for the disordered ligands. The mean Y–O bond length of the non-disordered dimethyl sulfoxide ligands in **1**, 2.36 Å (2.38 Å with riding motion correction assuming O to ride on Y), is close to the mean Y–O bond length 2.37 Å found for the octahydrated yttrium(III) ion in the solid $[Y(H_2O)_6]Cl_3 \cdot 15\text{-crown-5}$ compound, and in aqueous solution.^{5,36} Also, for the aqua ligands in the mixed complex $[Y(H_2O)_6(OSMe_2)_2]Cl_3$, the mean Y–O(aq) distance is 2.36 Å.³⁴

In the *N,N'*-dimethylpropyleneurea solvate the six oxygen atoms are octahedrally co-ordinated in the centrosymmetric $[Y(OCN_2Me_2(CH_2)_3)_6]^{3+}$ complex of compound **2** (Fig. 2) with the Y–O bond distances close to the mean value 2.22 Å (2.23 Å

Table 2 Crystallographic data for compounds **1** and **2**

	1	2
Formula	$C_{16}H_{48}I_3O_8S_8$	$C_{36}H_{72}I_3N_{12}O_6$
Formula weight	1094.63	1238.67
Crystal system	Monoclinic	Monoclinic
Space group (no.)	$P2_1/n$ (11)	$P2_1/n$ (11)
<i>T</i> /K	295	295
<i>a</i> /Å	12.3726(13)	12.1696(12)
<i>b</i> /Å	18.883(2)	12.1227(13)
<i>c</i> /Å	18.035(2)	17.9365(19)
β /°	99.977(2)	91.905(2)
<i>V</i> /Å ³	4149.8(8)	2644.7(5)
<i>Z</i>	4	2
μ (Mo–K α)/mm ^{–1}	4.070	2.902
No. of measured reflections	24595	15031
No. of independent reflections	9536	6078
<i>R</i> _{int} (θ _{max} /°)	0.091(56)	0.107(56)
<i>R</i> 1 [<i>I</i> > 2 σ (<i>I</i>)]	0.053	0.044
<i>wR</i> 2 [<i>I</i> > 2 σ (<i>I</i>)]	0.145	0.121

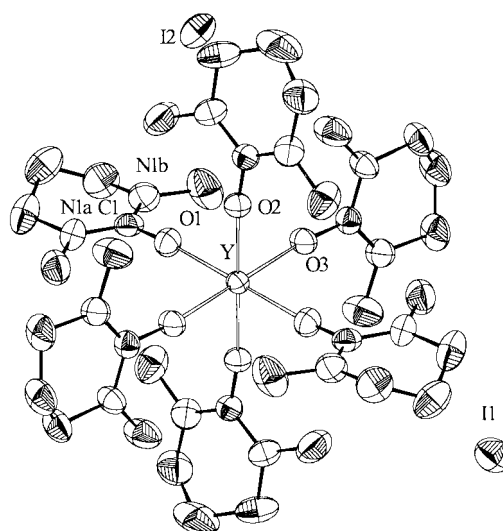


Fig. 2 Molecular structure of $[Y(OCN_2Me_2(CH_2)_3)_6]I_3$ **2**. Thermal ellipsoids are at 40% probability. Hydrogen atoms omitted for clarity. Distances (Å) are: Y–O(1) 2.215(3), Y–O(2) 2.221(3) and Y–O(3) 2.220(3). The mean Y...C distance is 3.47 Å.

after riding motion correction). The mean C–O distance of the urea ligands is 1.27 Å with the Y–O–C angles in the range 168 to 172°. This slight tilt of the bulky urea molecules is almost symmetrical as shown by the Y...N distances which are in the range 4.272 to 4.317 Å. There is no positional disorder in **2** and all the hydrogen atoms of the CH₃ and CH₂ groups could be located in a Fourier difference map. In the isomorphous $[Sc(OCN_2Me_2(CH_2)_3)_6]I_3$ structure the Sc–O–C angles are slightly larger, in the range 168.8 to 175.5° for the smaller Sc^{III} (mean Sc–O bond distance 2.074 Å).³⁷

LAXS study of yttrium(III) in dimethyl sulfoxide solution

The radial distribution function (RDF) of the dimethyl sulfoxide solution from the LAXS study is shown in Fig. 3. In addition to the two broad features around 5 and 10 Å arising from the bulk dimethyl sulfoxide structure,³¹ there are three major peaks below 4 Å corresponding to the distances within the solvated yttrium and trifluoromethanesulfonate ions. The C–F, S–O and C–S interactions from the trifluoromethanesulfonate ion and the S–O and C–S interactions from the dimethyl sulfoxide molecule are all contained within the broad unresolved peaks around 1.5 Å. The broad peak at about 2.5 Å corresponds to the Y–O bond interactions but also to the non-bonded interactions within the trifluoromethanesulfonate and dimethyl sulfoxide species. The sharp peak at 3.55 Å is due to

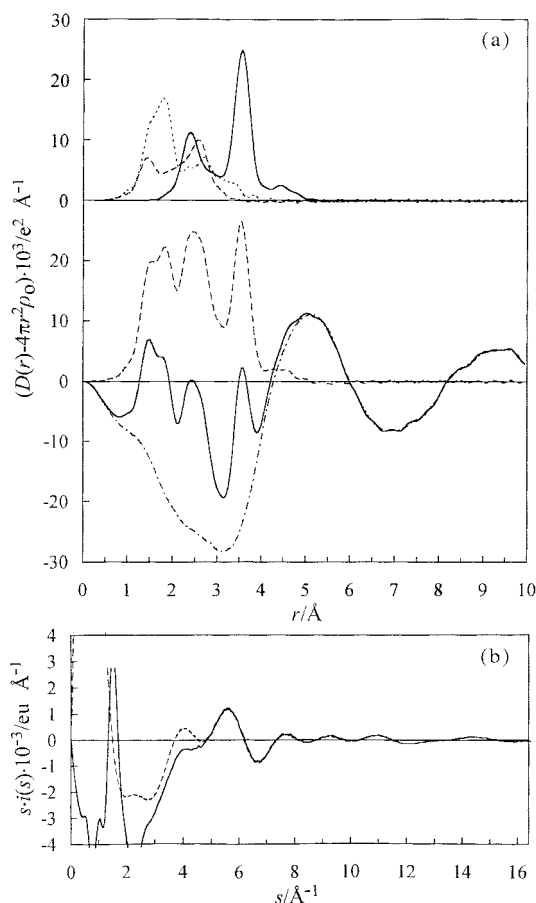


Fig. 3 LAXS radial distribution function (solid line) for $0.7 \text{ mol dm}^{-3} \text{ Y}(\text{CF}_3\text{SO}_3)_3$ in dimethyl sulfoxide. (a) The model curve (dashed line) is the sum of the intramolecular atom-pair interactions (Table 3), shown separately above: $\text{Y}-\text{O}_8$ and $\text{Y}\cdots\text{S}$ (solid line), CF_3SO_3^- (dashed line), Me_2SO solvent (dash-dotted line). (b) Experimental (solid line) and model (dashed line) $s \cdot i(s)$ intensity function in electron units.

the $\text{Y}\cdots\text{S}$ distance from the co-ordinated dimethyl sulfoxide molecules. The structural parameters for a model consisting of an YO_8 entity with an assumed square antiprismatic geometry and a $\text{Y}\cdots\text{S}$ mean distance were varied in least-squares refinements (Table 3). The mean $\text{Y}-\text{O}$ and $\text{Y}\cdots\text{S}$ distances obtained, $2.36(1)$ and $3.55(1) \text{ \AA}$, respectively, give an average $\text{Y}-\text{O}-\text{S}$ angle of about 131° (close to the crystal structure values of compound **1**) for an $\text{S}-\text{O}$ bond distance of 1.52 \AA in the co-ordinated dimethyl sulfoxide ligands.³¹ The fit of a model assuming nine-co-ordination in a tricapped trigonal prism is equally good, since the different $\text{O}\cdots\text{O}$ interactions within these two co-ordination polyhedra are overlapped with other distances, and therefore not possible to distinguish. However, the mean $\text{Y}-\text{O}$ bond distance obtained also for this model is typical for eight-co-ordination and excludes nine-coordination for which a significantly longer mean $\text{Y}-\text{O}$ distance would be expected.⁵⁻⁷

XAFS studies of the solvated yttrium(III) ion in solution

Edge structure. Similar featureless yttrium K-edges are found for the spectra of all the current samples (Fig. 4). However, the different multiple scattering contributions in the XANES region after the edge are obvious. The spectrum of the eight-co-ordinated solid dimethyl sulfoxide solvate **1** is very similar to that of the solvated yttrium(III) ion in dimethyl sulfoxide solution, and with only small differences from the spectrum of eight-co-ordinated yttrium ion in aqueous solution.⁵ Also, the spectrum of the N,N -dimethylformamide solution is similar, while that of the six-co-ordinated species in N,N' -dimethylpropyleneurea solution is strikingly different.

Table 3 LAXS model parameters for the solvated yttrium(III) ion in dimethyl sulfoxide solution **L4**

Interaction	n	$r/\text{\AA}$	$l/\text{\AA}$
$\text{Y}-\text{O}$	8	$2.364(6)$	$0.104(6)$
$\text{Y}\cdots\text{S}$	8	$3.550(2)$	$0.113(5)$

Parameters: n co-ordination number, r interatomic distance, l displacement parameter ($=2\sigma$). Estimated standard deviations from least-squares refinements are given in parentheses.

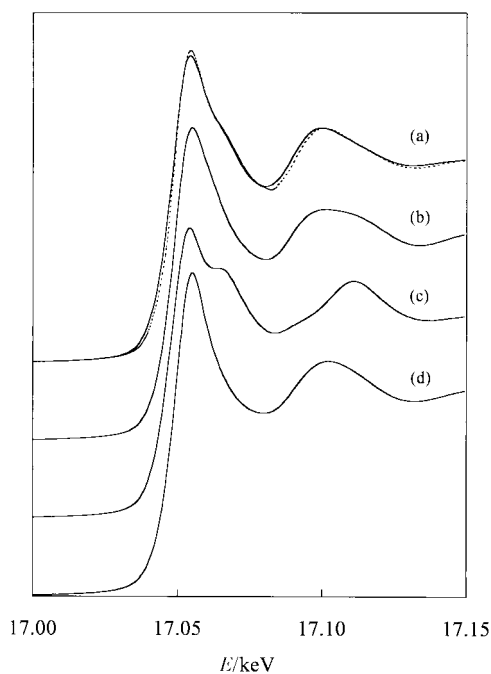


Fig. 4 Near edge structure (XANES) of the yttrium K absorption edges for (a) dimethyl sulfoxide solution (solid line) compared with that of compound **1** (dotted line), (b) N,N -dimethylformamide solution, (c) N,N' -dimethylpropyleneurea solution and (d) $1.7 \text{ mol dm}^{-3} \text{ Y}(\text{ClO}_4)_3$ aqueous solution (Ref. 5).

Dimethyl sulfoxide. The k^3 -weighted XAFS spectra and the corresponding Fourier transforms of the 1.0 mol dm^{-3} dimethyl sulfoxide solution and the crystalline solvate **1** are shown in Fig. 5(a) and (b), respectively. The close agreement between the spectra of the two samples is a strong indication of a similar local structure around yttrium. Thus, also for the solution a somewhat distorted square antiprism of the co-ordinated oxygen atoms, with a mean $\text{Y}-\text{O}$ bond distance of 2.36 \AA (Table 4), is the most probable arrangement. The second shell containing the sulfur atoms gives relatively large back-scattering amplitude. Assuming symmetric distributions, least-squares refinements gave the $\text{Y}-\text{O}$ and $\text{Y}\cdots\text{S}$ distances $2.354(3)$ and $3.54(1) \text{ \AA}$ for the solution, and $2.353(3)$ and $3.52(1) \text{ \AA}$ for the solid solvate **1**. The latter values are close to the mean distances $\text{Y}-\text{O}$ 2.36 \AA and $\text{Y}\cdots\text{S}$ 3.53 \AA obtained from the crystal structure determination of **1**, using only the atomic positions of the non-disordered ligands. The three-leg $\text{Y}-\text{O}-\text{S}$ multiple scattering path, which gives a contribution in opposite phase to that of the $\text{Y}\cdots\text{S}$ interaction in the low k region (Fig. 5), was refined to $3.71(1) \text{ \AA}$ for both samples. This corresponds to a mean $\text{Y}-\text{O}-\text{S}$ bond angle of 132° . The $\text{Y}-\text{O}-\text{O}$ paths within the YO_8 shell give weak contributions and were not included in the curve-fitting procedure. Fig. 5(c) and 5(d) show the fit of the model functions to the experimental k^3 -weighted XAFS data with the corresponding Fourier transforms, and separately the single back-scattering and multiple scattering contributions.

N,N -Dimethylformamide. The $\text{Y}-\text{O}$ bond distance obtained for the N,N -dimethylformamide solution, $2.35(1) \text{ \AA}$, is slightly

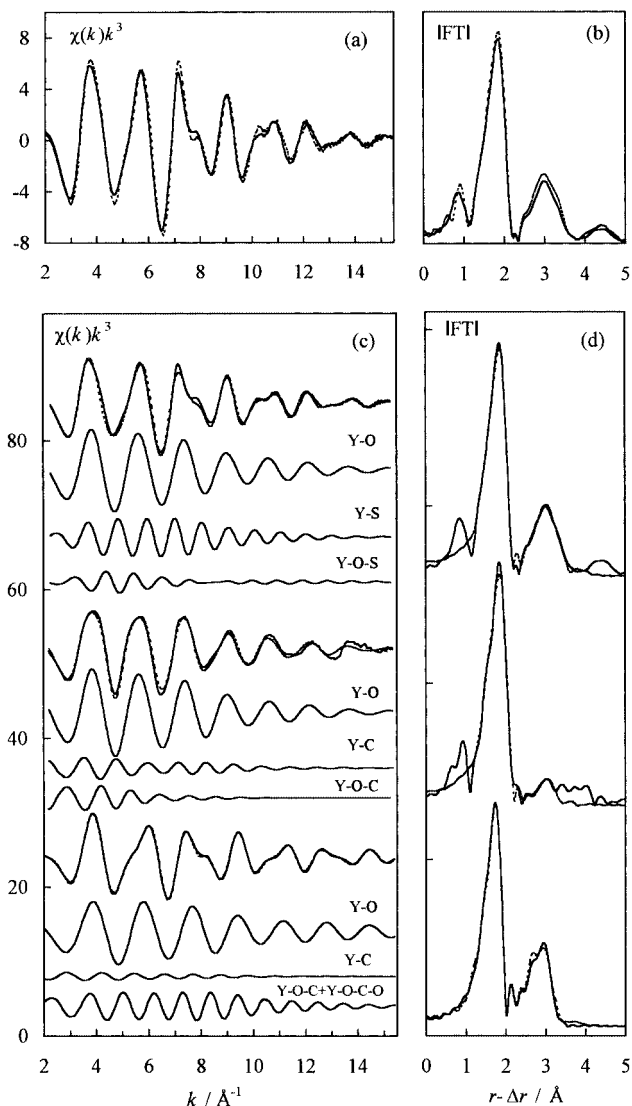


Fig. 5 (a) XAFS, k^3 -weighted experimental yttrium K-edge data: comparison of yttrium(III) in dimethyl sulfoxide solution (solid line) and compound **1** (dashed line). (b) Corresponding Fourier transforms. (c) Yttrium(III) in dimethyl sulfoxide **L1** (top), *N,N*-dimethylformamide **L2** (middle) and *N,N'*-dimethylpropyleneurea **L3** (bottom) solutions. Experimental (Fourier-filtered 0.7–4.2 Å) data (dashes) (for **L3**), model functions (solid line), and separate model contributions (see Table 4) below with solid lines. (d) Corresponding Fourier transforms.

shorter than that for dimethyl sulfoxide (Table 4). The $Y \cdots C$ peak in the Fourier transform is relatively small because of the destructive interference with the multiple scattering $Y-O-C$ path. The relative amplitudes (calculated from FEFF 8 with $\sigma^2 = 0$) of these two paths are both $\approx 30\%$ that of $Y-O$, but partly cancel each other due to opposing phases (Fig. 5c and 5d). However, the triangular $Y-O-C$ path length, 3.48(1) Å, gives a $C-O$ distance of 1.28(1) Å, close to the mean value 1.26 Å found for crystal structures with *N,N*-dimethylformamide molecules co-ordinated to trivalent ions.^{38,39} The $Y \cdots C$ distance obtained as 3.34(1) Å corresponds to an $Y-O-C$ angle of about 133°.

***N,N'*-Dimethylpropyleneurea.** The $Y-O$ bond distance for the solvated yttrium(III) ion in the *N,N'*-dimethylpropyleneurea solution was refined to 2.242(3) Å assuming a symmetrical distribution. The second prominent peak in the FT at 3.5 Å contains the contributions from the $Y \cdots C$ back scattering and the multiple scattering from the three-leg $Y-O-C$ and four-leg $Y-O-C-O$ paths (Fig. 5c, d). Curve fitting of the XAFS data, using single and multiple scattering paths for an octahedral configuration, gave a $Y \cdots C$ distance of 3.48(2) Å, in close

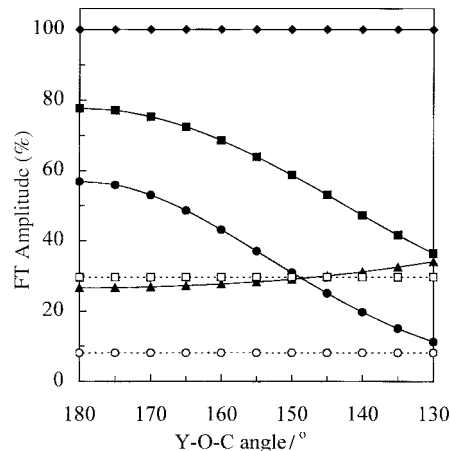


Fig. 6 The relative importance of individual scattering paths calculated (FEFF 8) for octahedral $Y(O-C)_6$ entities ($Y-O$ 2.24 Å, $O-C$ 1.27 Å) as a function of the $Y-O-C$ angle. The single scattering contributions are $Y-O$ (diamonds) and $Y \cdots C$ (triangles). Multiple scattering: $Y-O-C$ (squares), $Y-O-C-C$ (circles), $Y-O-C-O$ (open circles) and $Y-O-Y-O$ (open squares).

agreement with the mean value 3.47 Å from the crystal structure of **2**, for which the mean $Y-O-C$ angle is 169°. Owing to the almost linear $Y-O-C$ co-ordination geometry, the three-leg and four-leg scattering paths are only slightly longer than that of $Y \cdots C$, and these contributions were therefore constrained in the refinement procedure (see XAFS data analysis above). The mean $Y-O-C$ angle can be estimated to about 165° from the solution data using the distances $Y \cdots C$ 3.48, $Y-O$ 2.24 and $C-O$ 1.27 Å.

For an $Y-O-C$ angle of 165° the scattering intensities of the three- and four-leg paths, $Y-O-C$ and $Y-O-C-O$, are significantly enhanced, the so-called focusing effect. Fig. 6 shows the relative importance of the XAFS amplitude ratios for individual scattering paths calculated by FEFF 8 (see Experimental section) for an octahedral $Y(OC)_6$ entity as a function of the $Y-O-C$ angles. This shows that the amplitudes of the three- and four-leg paths are angle-sensitive, whereas those of $Y-O$, $Y \cdots C$, *cis*- $Y-O-O$ and *trans*- $Y-O-Y-O$ remain constant. Thus, the angle dependence contains information about the co-ordination angle, $Y-O-C$, to be obtained by comparing simulated XAFS spectra (FEFF 8) to the experimental spectrum of the *N,N'*-dimethylpropyleneurea solution. Theoretical spectra of octahedral $Y(OC)_6$ entities with $Y-O-C$ angles between 150 and 180° are shown in Fig. 6. At 150° the XAFS spectrum can be represented by the back scattering from the first co-ordination shell solely. The reason for this is destructive interference between the $Y \cdots C$ and $Y-O-C$ and $Y-O-C-O$ paths. At $Y-O-C$ angles larger than 160° the enhancement of the contribution from the three- and four-leg $Y-O-C$ and $Y-O-C-O$ pathways results in a more complex interference pattern. This comparison shows the XAFS spectra simulated for the $Y-O-C$ angles 160–170° to be most similar to the experimental one.

The calculated contributions for the linear pathways of $O-Y-O$ scattering of twice the bond length, which usually are significant for octahedral co-ordination (see Fig. 7, Ref. 40), are in this $Y(OC)_6$ configuration 0.09, 0.30 and 0.05 of the $Y-O$ contribution. However, they partly cancel and were not included.

Distribution of $Y-O$ bond distances. It was recently shown that the hydrated yttrium(III) ion, $[Y(H_2O)_9]^{3+}$, has a rather large spread of $Y-O$ bond distances in aqueous solution corresponding to a configurational disorder of about 0.1 Å, which gives rise to a fairly large Debye–Waller parameter $\sigma^2 = 0.0062(2)$ Å².⁵ In addition, a small but not insignificant asymmetry of the distribution was shown by a phase shift at high k values in the XAFS spectrum. When this was accounted

Table 4 XAFS model parameters for solvated yttrium(III) ions^a

Complex/medium	Sample	Path	<i>n</i>	<i>r</i> /Å	$\sigma^2/\text{\AA}^2$	$C_3/10^{-5} \text{\AA}^3$	$\Delta E_0/\text{eV}$	Residual ^b
[Y(OSMe ₂) ₈] ₃	1	Y–O ^c	8	2.356(3)	0.0069(4)	6(4)	0.0	6.2
		Y–O	8	2.353(3)	0.0069(4)		0.0(2)	6.9
		Y···S	8	3.52(1)	0.010(1)		0.0	
		Y–O–S ^d	6	3.71(1)	0.0070(4)		0.0	
Y(OSMe ₂) ₈ ³⁺ Me ₂ SO solution	L1	Y–O ^c	8	2.360(3)	0.0067(4)	12(4)	0.1	6.0
		Y–O	8	2.354(3)	0.0067(4)		0.1(2)	7.3
		Y···S	8	3.54(1)	0.011(1)		0.1	
		Y–O–S ^d	6	3.71(1)	0.0072(4)		0.1	
Y(OCHNMe ₂) ₆ ³⁺ <i>N,N</i> -Dimethylformamide solution	L2	Y–O ^c	8	2.355(3)	0.0069(4)	15(4)	–0.2	6.0
		Y–O	8	2.347(3)	0.0069(4)		–0.2(2)	7.2
		Y···C	8	3.34(1)	0.010(1)		–0.2	
		Y–O–C ^d	6	3.48(1)	0.0095(5)		–0.2	
Y(OCHN ₂ Me ₂ (CH ₂) ₃) ₃ ³⁺ <i>N,N'</i> -Dimethylpropyleneurea solution	L3	Y–O ^c	6	2.248(3)	0.0054(5)	12(4)	–0.2	10.2 (8.5) ^f
		Y–O	6	2.242(3)	0.0054(5)		–0.2(2)	12.4 (11.9) ^f
		Y···C	6	3.48(2)	0.0061(8)		–0.2	
		Y–O–C ^d	2	3.49 ^g	0.0061 ^g		–0.2	
		Y–O–C–O ^e	6	3.50 ^g	0.0061 ^g		–0.2	

^a Parameters: *n* frequency or co-ordination number, *r* scattering distance (half of pathway), σ^2 mean square displacement from mean distance, C_3 third cumulant. ΔE_0 shift of threshold energy. *k*-Space fitting (k^3 -weighted 2.0–15.5 Å^{–1}). ^b Residual (%) = $\sum_{i=1}^N [\chi_{\text{exp}}(i) - \chi_{\text{model}}(i)] / \sum_{i=1}^N \chi_{\text{exp}}(i)$.

^c *r*-Space fitting of Y–O shell (Fourier filtered 0–3.0 Å) including third cumulant, C_3 . ^d 3-Leg and ^e 4-leg multiple scattering. ^f *k*-Space refinement.

^g Correlated to the Y···C path (see text).

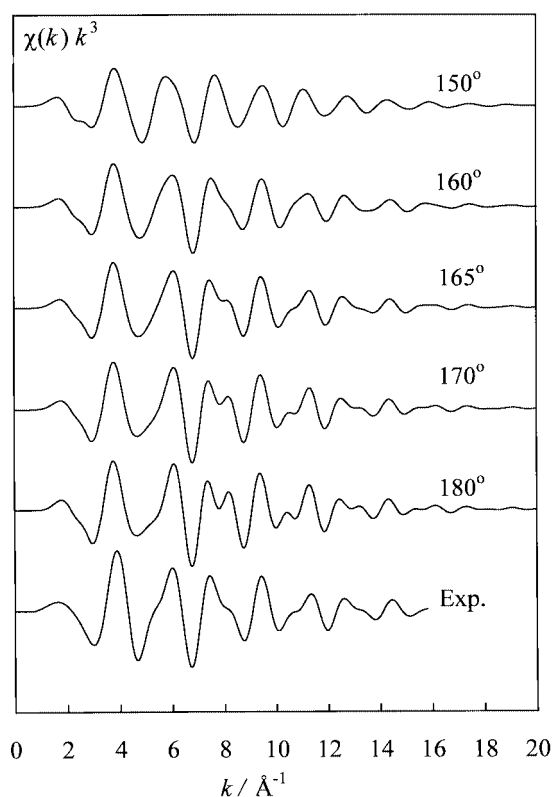


Fig. 7 XAFS simulations (FEFF 8) of octahedral Y(O–C)₆ entities with Y–O–C angles from 150 to 180°, compared to the experimental Fourier-filtered (0.7–4.2 Å) data of solvated yttrium(III) in *N,N'*-dimethylpropyleneurea solution **L3** (bottom curve). The theoretical model functions include all scattering paths of importance within a radius of 5 Å (see text).

for by using the cumulant expansion method the mean Y–O distance increased from 2.360 to 2.368 Å.⁵ The σ^2 parameters of the present eight-solvated [Y(Me₂SO)₈]³⁺ and [Y(dmf)₈]³⁺ complexes (Table 4) are slightly larger than that for the [Y(H₂O)₈]³⁺ ion, again reflecting a configurational disorder of similar magnitude. Such a disorder is also reflected by the σ^2 value of the three-leg paths, Y–O–S and Y–O–C, for which the refined values are smaller or similar to those of the corresponding

Y···S and Y···C paths. The cumulant expansion method was also applied on the XAFS data of the present samples, by means of *r*-space fitting of the Y–O peak. The fit improved somewhat by introducing the third cumulant, C_3 , and resulted in a slightly longer mean Y–O distance, see Table 4.

The importance of steric repulsion effects between the ligands has been shown in an XAFS study on the solvation of lanthanide(III) ions in *N,N*-dimethylformamide and *N,N*-dimethylacetamide.⁴ It was concluded that all lanthanides form eight-co-ordinated [Ln(dmf)₈]³⁺ species in *N,N*-dimethylformamide, but with the more bulky *N,N*-dimethylacetamide ligand, in which the formyl proton is replaced by a methyl group, the solvation number was proposed gradually to decrease from 8 to 7 from lanthanum to lutetium in the lanthanide series. For yttrium(III), with similar size to holmium(III), a solvation number close to seven would be expected in *N,N*-dimethylacetamide solution. In the *N,N'*-dimethylpropyleneurea molecule another methylated amide nitrogen has been attached to the carbonyl group and the steric ligand–ligand repulsion increases even further (*cf.* Scheme 1).

The solid *N,N'*-dimethylpropyleneurea solvate, **2**, shows an almost regular octahedral co-ordination in the [Y(OCN₂Me₂(CH₂)₃)₆]³⁺ species. The XAFS results for the solvated yttrium(III) ion in *N,N'*-dimethylpropyleneurea solution show the σ^2 parameter to be smaller than those for eight-co-ordinated yttrium(III) solvates, and indicate a more narrow distribution of the Y–O bond distances. Some asymmetry is indicated by the phase difference in the model fitting, and introduction of the third cumulant increases the mean Y–O distance to 2.248(3) Å. This is slightly longer than for the Y–O distances from the crystal structure, for which the average value becomes 2.23 Å, when corrected for thermal motion effects assuming riding motion. Conductometry (see Experimental section) showed, despite the strong solvating ability of *N,N'*-dimethylpropyleneurea, that ion pair formation between the triflate and the yttrium(III) ions occurs to some extent at the highest concentration, 0.25 mol dm^{–3} Y(CF₃SO₃)₃, in the saturated solution **L3**. The overlap with Y–solvent distances (Table 4) prevents any possibility to distinguish Y···S distances in the modelling of the EXAFS data, but ion pair formation is likely to increase the asymmetry of the distribution of the Y–O bond distances. Also, for octahedral co-ordination geometry no significant asymmetry effects due to ligand–ligand repulsion are expected. Therefore, the mean Y–O bond distance 2.242(3) Å, obtained assuming a

symmetric distribution, probably is more representative for the *N,N'*-dimethylpropyleneurea ligands. Recently, it was shown that triflate ions in methanol solutions form inner-sphere complexes replacing 1 or 2 methanol molecules of solvated dysprosium(III) ions.⁴¹

Conclusion

The yttrium(III) ion has similar Y–O bond distances, 2.36(1) Å, in dimethyl sulfoxide and *N,N*-dimethylformamide solution, respectively, most probably with eight-co-ordination in square antiprismatic configuration, while the *N,N'*-dimethylpropyleneurea solvated yttrium ion has a mean Y–O bond distance of 2.24(1) Å in *N,N'*-dimethylpropyleneurea solution, probably with an octahedral co-ordination geometry as in the solid solvate. The asymmetry found in the distribution of the Y–O distances in solution is presumably caused by ion-pair formation with the triflate ions, but this could not be modelled in detail with the XAFS data available. The difference in the Y–O bond distances for the six- and eight-co-ordinated yttrium species is 0.12 Å as predicted by Shannon's ionic radii.⁶

The *N,N'*-dimethylpropyleneurea molecule co-ordinates via the oxygen atom of an O=C–N unit in a similar way as for *N,N*-dimethylformamide (Scheme 1), and comparable bond properties could be expected. However, the two methyl groups near the oxygen atom make the co-ordinated urea molecule more space-requiring than dimethyl sulfoxide or *N,N*-dimethylformamide, which is the reason for the observed decrease in the co-ordination number from eight to six. Moreover, the Y–O–C angle seems to depend on steric requirements. For the [Sc(OCN₂Me₂(CH₂)₃)₃]₃I₃ and [Y(OCN₂Me₂(CH₂)₃)₃]₃I₃ compounds with mean metal–oxygen bond distances of 2.07 and 2.22 Å, the mean M–O–C angles are 172 and 169°, respectively.³⁷ For the larger but likewise seven-co-ordinated lanthanum(III) ion in *N,N'*-dimethylpropyleneurea solution, the La–O–C angle is 149° for La–O 2.45 Å.¹⁷ Thus, the M–O–C angle decreases significantly when the size of the metal ion increases.

Acknowledgements

We gratefully acknowledge the Swedish Natural Science Research Council for financial support and the Stanford Synchrotron Radiation Laboratory (SSRL) for allocation of beam time and laboratory facilities. SSRL is operated by the Department of Energy, Office of Basic Energy Sciences. The SSRL Biotechnology Program is supported by the National Institutes of Health, National Centre for Research Resources, Biomedical Technology Program, and by the Department of Energy, Office of Biological and Environmental Research.

References

- 1 S. Ishiguro, Y. Umebayashi, K. Kato, S. Nakasone and R. Takahashi, *Phys. Chem. Chem. Phys.*, 1999, **1**, 2725.
- 2 G. Johansson, H. Yokoyama and H. Ohtaki, *J. Solution Chem.*, 1991, **20**, 859.
- 3 G. Johansson, *Adv. Inorg. Chem.*, 1992, **39**, 159.
- 4 S. Ishiguro, K. Kato, R. Takahashi and S. Nakasone, *Rare Earths*, 1995, **11**, 61.
- 5 P. Lindqvist-Reis, K. Lamble, S. Pattanaik, I. Persson and M. Sandström, *J. Phys. Chem. B*, 2000, **104**, 402.
- 6 R. D. Shannon, *Acta Crystallogr., Sect. A*, 1976, **32**, 751.
- 7 J. M. Harrowfield, D. L. Kepert, J. M. Patrick and A. H. White, *Aust. J. Chem.*, 1983, **36**, 483.
- 8 J. Glaser and G. Johansson, *Acta Chem. Scand., Ser. A*, 1981, **35**, 639.
- 9 T. G. Cherkasova, *Zh. Neorg. Khim.*, 1994, **39**, 1316.
- 10 M. Klinga, R. Cuesta, J. M. Moreno, J. M. Dominguez-Vera, E. Colacio and R. Kivekas, *Acta Crystallogr., Sect. C*, 1998, **54**, 1275.
- 11 Q. Huang, X. Wu, Q. Wang, T. Sheng and J. Lu, *Angew. Chem., Int. Ed. Engl.*, 1996, **35**, 868.
- 12 D. T. Richens, in *The Chemistry of Aqua Ions*, Wiley, Chichester, 1997, ch. 3.
- 13 Th. Kowall, F. Foglia, L. Helm and A. E. Merbach, *J. Phys. Chem.*, 1995, **99**, 13078.
- 14 Product information from BASF: cf. <http://www.basf-ag.basf.de/en/produkte/chemikalien/interm/czuche/> for CAS no. 7226-23-5, *N,N'*-dimethylpropyleneurea (systematic name: tetrahydro-1,3-dimethyl-1H-pyrimidin-2-one).
- 15 L. Weng and I. Persson, unpublished work.
- 16 M. Sandström, I. Persson and P. Persson, *Acta Chem. Scand.*, 1990, **44**, 653.
- 17 J. Näslund, P. Lindqvist-Reis, I. Persson and M. Sandström, *Inorg. Chem.*, 2000, **39**, in press.
- 18 I. Persson, M. Sandström, H. Yokoyama and M. Chaudhry, *Z. Naturforsch., Teil A*, 1995, **50**, 21.
- 19 J. E. Roberts and J. S. Bykowski, *Thermochim. Acta*, 1978, **25**, 233.
- 20 G. Schwarzenbach and H. Flaschka, *Die Komplextometrische Titration*, Ferdinand Enke, Stuttgart, 1965.
- 21 SMART, 5.046 (area detector control), SAINT, 5.01 (integration software), SADABS (empirical absorption correction), SHELXTL, 5.1, Bruker Analytical X-Ray Systems, Madison, WI, 1998.
- 22 G. N. George and I. J. Pickering, EXAFSPAK, A Suite of Computer Programs for Analysis of X-Ray Absorption Spectra, SSRL, Stanford, CA, 1993.
- 23 T. Ressler, *J. Synchr. Rad.*, 1998, **5**, 118.
- 24 S. I. Zabinsky, J. J. Rehr, A. Ankudinov, R. C. Albers and M. J. Eller, *Phys. Rev. B*, 1995, **52**, 2995; A. Ankudinov, Ph.D. Thesis, University of Washington, 1996; J. J. Rehr, A. Ankudinov and S. I. Zabinsky, *Catal. Today*, 1998, **39**, 263.
- 25 FEFF code for ab initio calculations of XAFS: <http://feff.phys.washington.edu/feff>.
- 26 H. Zhang, B. Hedman and K. O. Hodgson in *Inorganic Electronic Structure and Spectroscopy*, ed. E. I. Solomon and A. B. P. Lever, John Wiley and Sons, New York, 1999, vol. I, ch. 9.
- 27 E. D. Crozier, J. J. Rehr and R. Ingalls, in *X-Ray Absorption, Principles, Applications, Techniques of EXAFS, SEXAFS, and XANES*, ed. D. C. Koningsberger and R. Prins, Wiley-Interscience, New York, 1988, ch. 9.
- 28 G. Bunker, *Nucl. Instrum. Methods*, 1983, **207**, 437.
- 29 C. M. V. Stålhandske, I. Persson, M. Sandström and E. Kamienska-Piotrowicz, *Inorg. Chem.*, 1997, **36**, 3174, and references therein.
- 30 G. Nieuwpoort, G. C. Verschoor and J. Reedijk, *J. Chem. Soc., Dalton Trans.*, 1983, 531.
- 31 S. Åhrland, E. Hansson, Å. Iverfeldt and I. Persson, *Acta Chem. Scand., Ser. A*, 1981, **35**, 275.
- 32 G. Johansson and M. Sandström, *Chem. Scr.*, 1973, **4**, 195.
- 33 M. Molund and I. Persson, *Chem. Scr.*, 1985, **25**, 197.
- 34 O. Kristiansson and P. Lindqvist-Reis, *Acta Crystallogr., Sect. C*, 2000, **56**, 163.
- 35 M. Calligaris and O. Carugo, *Coord. Chem. Rev.*, 1996, **153**, 83.
- 36 R. D. Rogers and L. K. Kurihara, *Inorg. Chim. Acta*, 1986, **116**, 171.
- 37 P. Lindqvist-Reis, O. Kristiansson, S. Pattanaik, I. Persson and M. Sandström, unpublished work.
- 38 W. Levason, J. J. Quirk and G. Reid, *Acta Crystallogr., Sect. C*, 1997, **53**, 1224.
- 39 H. Suzuki and S. Ishiguro, *Acta Crystallogr., Sect. C*, 1998, **54**, 586.
- 40 P. Lindqvist-Reis, A. Muñoz-Páez, S. Díaz-Moreno, S. Pattanaik, I. Persson and M. Sandström, *Inorg. Chem.*, 1998, **37**, 6675.
- 41 A. M. van Loon, H. van Bekkum and J. A. Peters, *Inorg. Chem.*, 1999, **28**, 3080.